Effects of systemic multiexon skipping with peptide-conjugated morpholinos in the heart of a dog model of Duchenne muscular dystrophy

Yusuke Echigoya[a], Akinori Nakamura[b,c], Tetsuya Nagata[b], Nobuyuki Urasawa[b,d], Kenji Rowel Q. Lim[a], Nhu Trieu[a], Dharminder Panesar[a], Mutsuki Kuraoka[b], Hong M. Moulton[e], Takashi Saito[b], Yoshitsugu Aoki[b], Patrick Iversen[f], Peter Sazani[f], Ryszard Kole[f], Rika Maruyama[a], Terry Partridge[g,h], Shin'ichi Takeda[b,1], and Toshifumi Yokota[a,i,1]

[a]Department of Medical Genetics, School of Human Development, Faculty of Medicine and Dentistry, University of Alberta, Edmonton, AB, Canada T6G 2H7; [b]Department of Molecular Therapy, National Center of Neurology and Psychiatry, National Institute of Neuroscience, Kodaira, Tokyo 187-8502, Japan; [c]Third Department of Internal Medicine, Shinshu University School of Medicine, Matsumoto, Nagano 390-8621, Japan; [d]Department of Cardiovascular Internal Medicine, Nagano Red Cross Hospital, Nagano 380-8582, Japan; [e]Department of Biomedical Sciences, College of Veterinary Medicine, Oregon State University, Corvallis, OR 97331; [f]Sarepta Therapeutics, Inc., Cambridge, MA 02142; [g]Research Center for Genetic Medicine, Children's National Medical Center, Washington, DC 20010; [h]Department of Integrative Systems Biology, George Washington University School of Medicine, Washington, DC 20010; and [i]The Friends of Garrett Cumming Research & Muscular Dystrophy Canada HM Toupin Neurological Science Research Chair, Edmonton, AB, Canada T6G 2H7

Duchenne muscular dystrophy (DMD) is a lethal genetic disorder caused by an absence of the dystrophin protein in bodywide muscles, including the heart. Cardiomyopathy is a leading cause of death in DMD. Exon skipping via synthetic phosphorodiamidate morpholino oligomers (PMOs) represents one of the most promising therapeutic options, yet PMOs have shown very little efficacy in cardiac muscle. To increase therapeutic potency in cardiac muscle, we tested a next-generation morpholino: arginine-rich, cell-penetrating peptide-conjugated PMOs (PPMOs) in the canine X-linked muscular dystrophy in Japan (CXMD_J) dog model of DMD. A PPMO cocktail designed to skip dystrophin exons 6 and 8 was injected intramuscularly, intracoronarily, or intravenously into CXMD_J dogs. Intravenous injections with PPMOs restored dystrophin expression in the myocardium and cardiac Purkinje fibers, as well as skeletal muscles. Vacuole degeneration of cardiac Purkinje fibers, as seen in DMD patients, was ameliorated in PPMO-treated dogs. Although symptoms and functions in skeletal muscle were not ameliorated by i.v. treatment, electrocardiogram abnormalities (increased Q-amplitude and Q/R ratio) were improved in CXMD_J dogs after intracoronary or i.v. administration. No obvious evidence of toxicity was found in blood tests throughout the monitoring period of one or four systemic treatments with the PPMO cocktail (12 mg/kg/injection). The present study reports the rescue of dystrophin expression and recovery of the conduction system in the heart of dystrophic dogs by PPMO-mediated multiexon skipping. We demonstrate that rescued dystrophin expression in the Purkinje fibers leads to the improvement/prevention of cardiac conduction abnormalities in the dystrophic heart.

Duchenne muscular dystrophy | exon skipping | peptide-conjugated morpholinos | cardiac Purkinje fibers | dystrophic dog model

Duchenne muscular dystrophy (DMD) is the most common lethal myopathy, and is characterized by progressive muscle degeneration and weakness (1). Patients typically die around 20–30 y of age because of cardiac and/or respiratory failure. DMD is caused by a lack of dystrophin protein due to mutations in the dystrophin gene (2). Exon skipping using a splice-switching oligonucleotide (SSO) is one of the most promising therapies for DMD and is currently the focus of clinical trials (3). SSO-mediated exon skipping prevents the incorporation of mutated exons and/or neighboring exons into the spliced mRNA and restores its reading frame (4). As a result, internally deleted but partly functional dystrophin protein is produced from the modified mRNA, similar to what is observed in the milder dystrophinopathy, Becker muscular dystrophy (BMD) (5, 6).

Therapeutic exon skipping that targets a single exon is applicable to 64% of all DMD patients (7). Multiexon skipping can potentially increase the scope of SSO therapy to ~90% of deletion mutations, 80% of duplication mutations, and 98% of nonsense mutations (8, 9). In some cases, efficient exon skipping is induced using a few SSOs targeting different positions in the same exon (10, 11). Thus, SSOs need to be designed according to mutation patterns and/or the nature of the target exon. Golden Retriever muscular dystrophy (GRMD) and beagle-based canine X-linked muscular dystrophy in Japan (CXMD_J), in which the dystrophin reading frame can be restored by skipping exons 6 and 8 (Fig. 1A), are widely accepted as adequate animal models to examine the potential of multiexon skipping (12). Previously, we demonstrated that a cocktail of SSOs targeting exons 6 and 8 efficiently induced multi-exon skipping and rescued dystrophin expression in bodywide skeletal muscles (10).

Although antisense phosphorodiamidate morpholino oligomers (PMOs) effectively rescued dystrophic phenotypes in murine and canine models and were well tolerated in patients enrolled in clinical trials (3), they were inefficient in cardiac muscles (10, 13). Only minuscule levels of rescued dystrophin protein have been

Significance

Duchenne muscular dystrophy (DMD) is a lethal genetic disorder caused by a lack of dystrophin protein. Cardiomyopathy is a leading cause of death in DMD. Although exon skipping with antisense morpholino oligonucleotides is very promising, morpholino-mediated exon skipping has induced barely detectable dystrophin levels in the hearts of DMD animal models. Here, we show that systemic multiexon skipping using a cocktail of peptide-conjugated morpholinos (PPMOs) rescued dystrophin expression in the myocardium and cardiac Purkinje fibers in a dystrophic dog model. The treatment reduced vacuole degeneration in Purkinje fibers and improved electrocardiogram abnormalities without apparent toxicity. These results indicate that PPMO-mediated multiexon skipping is a therapeutic approach for treating cardiac conduction abnormalities in DMD.
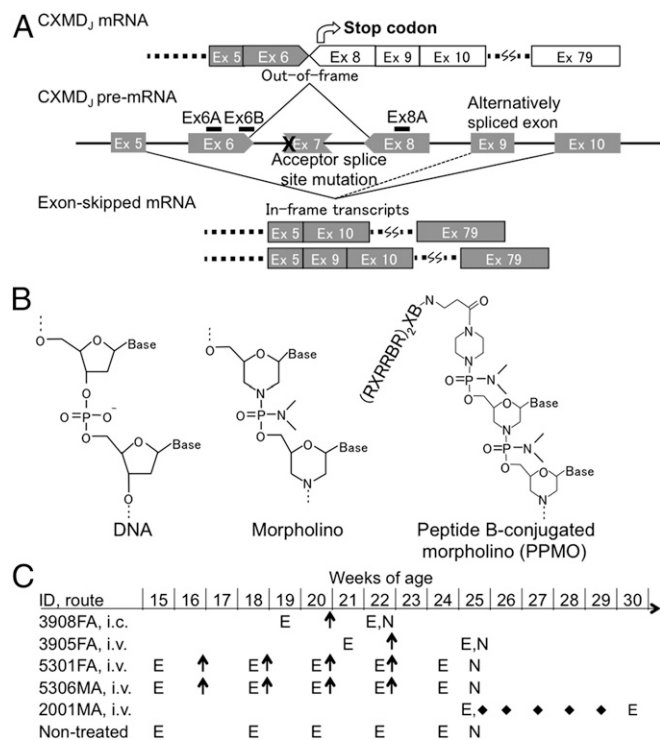
MEDICAL SCIENCES

Fig. 1. Therapeutic strategy with multiple exon skipping using the 3-PPMO cocktail in CXMD_J dogs. (*A*) The splice site mutation and design of splice-switching oligonucleotides (Ex6A, 6B, and Ex8A) for simultaneous skipping of exons 6 and 8. Exon 7 is spontaneously spliced out due to the mutation. (*B*) PPMO chemistry with peptide B sequence: B, β-alanine; R, ʟ-arginine; X, 6-aminohexanoic acid. (*C*) Schematic outline of PPMO or unmodified PMO treatment in affected dogs. E, electrocardiogram; FA, female-affected; i.c., intracoronary artery injection; i.v., i.v. injection; MA, male-affected; N, necropsy; arrows, injections of a 3-PPMO cocktail (12 mg/kg/injection, 4 mg/kg each); diamonds, injections of a 3-ummodified PMO cocktail (120 mg/kg/injection, 40 mg/kg each).

reported in dystrophin-deficient hearts of animal models following exon skipping using unmodified morpholinos. Adeno-associated virus vector-mediated gene therapy has enabled induction of mini-dystrophin in the heart of a dystrophic dog model (14, 15). As another promising solution, PMOs conjugated with cell-penetrating peptides (CPPs) have been developed to induce dystrophin expression more effectively in bodywide muscles including the heart (16–19). However, it is still unclear if cardiac conduction abnormalities as detected by electrocardiography (ECG) in DMD patients can be improved by the rescue of dystrophin expression in the heart. Although dystrophic mouse models show few cardiac abnormalities (20), dystrophic dog models, particularly CXMD_J dogs, manifest obvious cardiac symptoms, including distinct Q-waves and increased Q/R ratio, which indicate a cardiac conduction abnormality, in ECG (21), and vacuole degeneration in cardiac Purkinje fibers by 4 mo of age (22). We report here that systemic treatment with a cocktail of peptide-conjugated morpholinos (PPMOs) (18) (Fig. 1 *B* and *C*) results in successful skipping of multiple targeted exons, which restores expression of dystrophin protein in both skeletal and cardiac muscles in dystrophic dogs and ameliorates cardiac conduction defects. Blood tests indicate no obvious evidence of toxicity during follow-up of systemic treatment with one or four i.v. injections of the PPMO cocktail.

Results

Intramuscular Injection of the 3-PPMO Cocktail into Skeletal Muscle of the CXMD_J Dog. The efficacy of the 3-PPMO cocktail (Ex6, Ex6B, and Ex8A) to skip exons 6 and 8 was initially tested by a single intramuscular injection into the cranial tibialis muscles of CXMD_J dogs (Fig. S1): dogs 3908 female-affected (FA) and 3905FA were intramuscularly treated with 3-PPMOs and negative controls of either Ex6A only or saline, respectively. Two weeks after injection with a total of either 3,600 μg or 1,200 μg of the cocktail PPMOs (i.e., 1,200 μg or 400 μg of Ex6A, Ex6B, and Ex8A each, respectively), high-efficiency skipping of exons 6 and 8 was induced as shown by RT-PCR analysis (Fig. S1*A*). Removal of exons 6 and 8 was confirmed by sequencing of the PCR product (Fig. S1*B*). Western blotting demonstrated that intramuscular injection with the PPMO cocktail effectively rescued dystrophin protein expression, accompanied by increased levels of a dystrophin-associated protein, β-dystroglycan (Fig. S1 *C* and *D*). In immuno-histochemistry, extensive expression of dystrophin-positive fibers (more than 93%) was observed in the CXMD_J dog (3908FA) after treatment with both doses (Fig. S1 *E* and *F*).

A Single Intracoronary Artery or i.v. Injection of the 3-PPMO Cocktail. To examine whether dystrophin expression can be induced in cardiac muscles by multiple exon skipping, we injected the 3-PPMO cocktail (12 mg/kg total, 4 mg/kg each of Ex6A, Ex6B, and Ex8A) into two CXMD_J dogs (ID no. 3908FA and 3905FA) at 5 mo of age through two different administration routes: (*i*) intracoronary artery (i.c.) and (*ii*) i.v. injections, respectively. Two weeks after a single injection via either route, exons 6–9 skipped in-frame dystrophin transcripts were observed in cardiac muscles (Fig. 2 *A* and *B*). Western blotting analysis revealed increased expression levels of rescued dystrophin protein in most areas of the heart following single-dose treatment with the 3-PPMO cocktail (Fig. 2 *C* and *D*).

Efficacy of Four Consecutive Systemic Treatments with the 3-PPMO Cocktail in Skeletal Muscles. To examine the systemic effects of extended treatment with the 3-PPMO cocktail, we intravenously injected 12 mg/kg total PPMO (4 mg/kg each PPMO) into two CXMD_J dogs [ID no. 5301FA and 5306 male-affected (MA)] four times at 2-wk intervals. RT-PCR analysis revealed expression
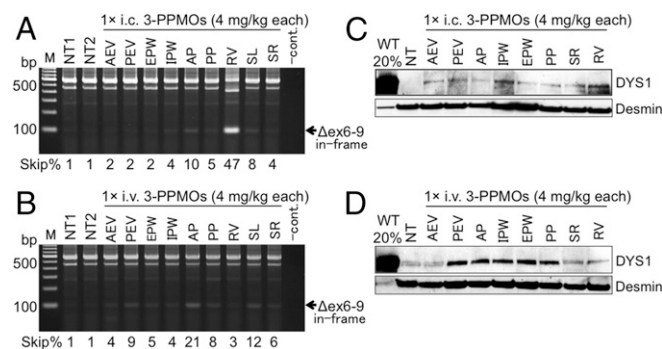

Fig. 2. Multiexon skipping and rescued dystrophin in the heart of CXMD_J dogs after a single i.c. or i.v. injection with the 3-PPMO cocktail (12 mg/kg total, 4 mg/kg each PPMO). (*A* and *B*) Exons 6–9 skipped dystrophin transcripts in the heart of the CXMD_J dog model treated with a single i.c. or i.v. injection, respectively. Exon 9 is spontaneously spliced out along with exons 6 and 8 skipping without affecting the reading frame. Western blotting with the anti-dystrophin rod domain antibody (DYS1) shows dystrophin restoration in the dystrophic heart following one i.c. (*C*) or i.v. (*D*) treatment with the 3-PPMOs. Forty micrograms of protein was loaded for nontreated (NT) and treated dog muscle samples. In wild-type (WT) dogs, 8 μg (20%) of protein was loaded as a positive control. Anti-desmin antibody was used as a loading control. Positive bands in NT dog samples indicate revertant fiber-derived dystrophin expression. AEV, anterior external area of the left ventricle (LV); AP, anterior papillary; EPW, endocardial surface of the posterior wall of LV; IPW, inferoposterior wall of LV; PEV, posterior external area of LV; PP, posterior papillary; RV, right ventricle; SL, the left side of the interventricular septum (IVS); SR, the right side of IVS.
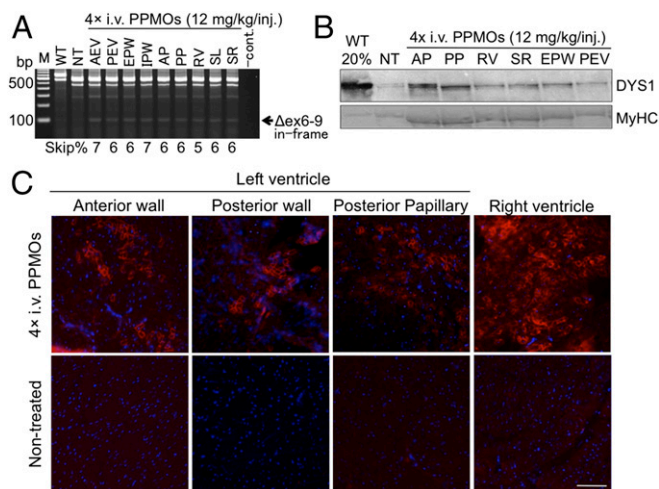
Fig. 3. Recovery of dystrophin expression in working myocardium 2 wk after four i.v. injections of the 3-PPMO cocktail (12 mg/kg/i.v.) into CXMD$_J$ dogs (5301FA and 5306MA). (*A*) The efficiency of exons 6–9 skipping in the cardiac tissues. (*B*) Western blotting following four i.v. injections at 2-wk intervals. Myosin heavy chain (MyHC) on a posttransferred gel is shown as a loading control. (*C*) Immunohistochemistry with the NCL-DYS1 antibody (red). Nuclei were counterstained with DAPI (blue). (Scale bar, 100 μm.) Representative images are shown.

of in-frame dystrophin mRNA, in which exons 6–9 were skipped, in skeletal muscles of the affected dogs after consecutive i.v. treatments with the 3-PPMO cocktail (Fig. S2*A*). An increase in dystrophin protein levels (∼5% of the wild-type dog) was confirmed in most skeletal muscles of the treated dogs by Western blotting (Fig. S2*B*). In immunohistochemistry, extensive expression of dystrophin-positive fibers was observed throughout skeletal muscles after systemic treatment with the PPMO cocktail (Fig. S2*C*). The number of centrally nucleated fibers (CNFs) present in muscle tissue, indicative of cycles of muscle degeneration and regeneration, was examined by hematoxylin/eosin (H&E) staining. Although the percentage of CNFs in wild-type dogs was a mean 0.05% ± 0.07 (SD) with six skeletal muscle types tested (*n* = 3– 5 for each type), affected dogs had CNFs at 11.3% ± 1.4% on average with the six muscle types. A reduced percentage of CNFs was observed in most areas of skeletal muscles in PPMO-treated dogs (Fig. S2 *D* and *E*): mean 4.6% ± 1.5% and 3.0% ± 1.0% in six tested skeletal muscle types of dogs 5301FA and 5306MA, respectively. However, no improvement in the clinical grading or muscle function was observed in the treated dogs (Fig. S2 *F* and *G*). Spontaneous locomotor activity showed no apparent change in treated dogs compared with nontreated affected dogs over 5 d/nights 1 wk after the final injection (Fig. S2*H*).

Restoration of Dystrophin Expression in Myocardium After Four Systemic Administrations of the 3-PPMO Cocktail. Exons 6–9 skipped in-frame dystrophin transcripts were detected in most areas of the cardiac muscle in consecutively treated CXMD$_J$ dogs 5301FA and 5306MA (Fig. 3*A*). Western blotting analysis revealed increased levels of dystrophin protein with a molecular weight of ∼400 kDa in the heart (∼5% dystrophin protein compared with that of the wild-type dog) (Fig. 3*B*). In immunohistochemistry, scattered dystrophin-positive fibers were extensively observed in the working myocardium 2 wk after the final i.v. injection (Fig. 3*C*).

Recovery of Dystrophin Expression and Amelioration of Vacuole Degeneration in Cardiac Purkinje Fibers in CXMD$_J$ Dogs. CXMD$_J$ dogs have been reported to exhibit vacuole degeneration in cardiac Purkinje fibers, a histopathological finding also seen in

DMD patients (22–24). We examined whether rescued dystrophin expression can ameliorate vacuole degeneration in CXMD$_J$ dogs. Cardiac Purkinje fibers were identified as having a larger diameter and fainter stainability compared with working myocardium, as observed on transverse sections following H&E staining, as previously described (22). Immunohistochemistry and H&E staining of serial sections revealed reduced vacuole degeneration in cardiac Purkinje fibers, which was accompanied by the recovery of dystrophin expression in the same fibers, of the systemically treated CXMD$_J$ dogs (ID nos. 5301FA and 5306MA), whereas large and many vacuoles were observed in Purkinje fibers of nontreated CXMD$_J$ dogs (Fig. 4*A*). In all regimens tested, amelioration of vacuole degeneration in Purkinje fibers was found in all four treated CXMD$_J$ dogs, and a statistically significant difference in the vacuole areas was found between treated and nontreated dog groups (Fig. 4*B*). In the heart of nontreated CXMD$_J$ dogs, degenerative vacuole areas of up to 24% of cardiac Purkinje fiber regions were observed. After a single administration of the PPMO cocktail through i.c. or i.v. injection, the area of vacuole degeneration was reduced to ∼13% and 7%, respectively. In the two CXMD$_J$ dogs subjected to four
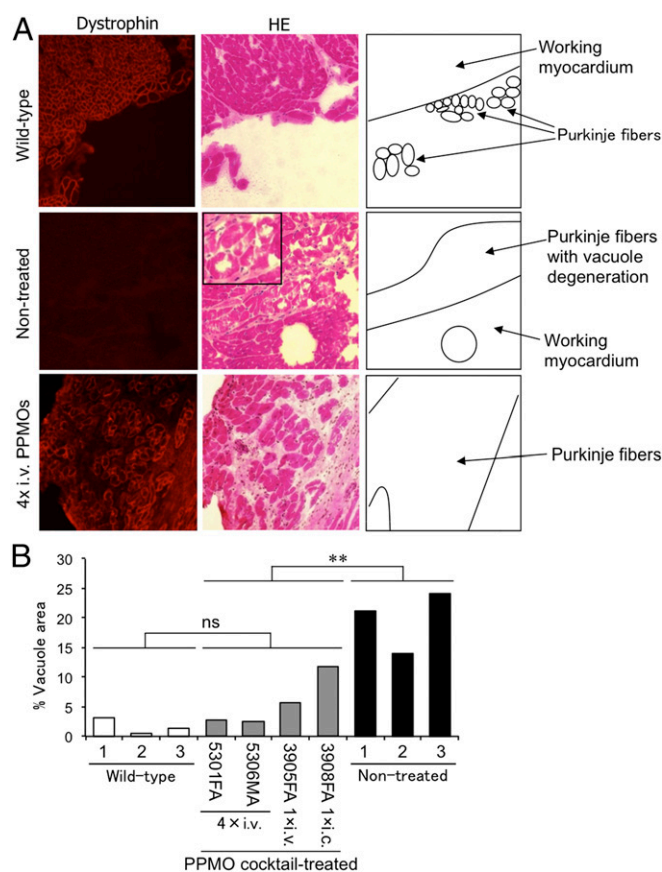

Fig. 4. Ameliorated histology of cardiac Purkinje fibers in dystrophic dogs 2 wk after a single injection or four systemic injections with the 3-PPMO cocktail (12 mg/kg/injection). (*A*) Dystrophin expression by immunohistochemistry (*Left* panels) and H&E staining (*Middle* panels) with serial sections and drawn schemes of the Purkinje fibers (*Right* panels). Purkinje fibers are shown in the peripheral area of the cardiac muscle tissue with faint stainability in H&E staining. (*Inset*) A magnified instance of vacuole degeneration in nontreated dogs. Representative images with the four i.v.-treated CXMD$_J$ dogs and nontreated affected dogs are shown. (*B*) The relative area of vacuole degeneration in cardiac Purkinje fibers after PPMO treatment by i.c. or i.v. injection. ns, no significant difference. **$P < 0.01$ between treated and nontreated groups (Student's *t* test).

systemic injections at 2-wk intervals with the 3-PPMO cocktail, we observed amelioration of degenerative Purkinje fibers to less than 3% of the vacuole area, comparable to the vacuole area in wild-type dogs.

Amelioration of Cardiac Conduction Abnormalities in CXMD$_J$ Dogs After Treatment with the 3-PPMO Cocktail. Cardiac conduction disturbance in CXMD$_J$ and GRMD dogs becomes clinically evident using ECG, demonstrated by deep and narrow Q-waves, which are reported in DMD patients (21, 25–27). The dystrophic dog models have also been reported to manifest increased Q/R ratio as an outcome of impaired cardiac function (21, 25). To assess recovery of the cardiac conduction system after treatment with the 3-PPMO cocktail (12 mg/kg, 4 mg/kg each), ECG with lead II was analyzed in CXMD$_J$ dogs before and after the single i.v. or i.c. injection or after the four i.v. injections at 2-wk intervals. A peak of distinct Q-waves and a high Q/R ratio outside the normal range were observed by 4 mo of age in nontreated dogs and three dogs subjected to treatment; therefore, injection with the PPMO or PMO cocktail was initiated at 4–5 mo of age. ECG abnormalities (deep Q-amplitude and Q/R ratio) were confounded in the control dog systemically treated with 3-unmodified PMO cocktail (120 mg/kg, 40 mg/kg each) even after five weekly injections (Fig. 5 *A* and *B*). In contrast, abnormal ECG findings were improved in three treated CXMD$_J$ dogs that manifested abnormal ECG before the treatment: dog 3908FA by 1× i.c., dog 3905FA by 1× i.v., and dog 5301FA by 4× i.v. The Q-amplitude and Q/R ratio of the CXMD$_J$ dog 5306MA, which did not manifest ECG abnormality before the treatment, remained in the normal range 2 wk after the final injection. In echocardiography (echo) tests, no abnormal findings were found in left ventricular size, shape, and contractility in the hearts of all four

dogs before treatment compared with reference values (21, 28): left ventricular internal diameter (LVID) in diastole (LVIDd), 24.1 mm ± 3.4 (SD); LVID in systole (LVIDs), 14.1 mm ± 1.8; interventricular septum thickness in diastole (IVSd), 5.6 mm ± 0.9; interventricular septum thickness in systole (IVSs), 9.1 mm ± 1.4; left ventricular posterior wall thickness in diastole (LVPWd), 5.3 mm ± 0.7; left ventricular posterior wall thickness in systole (LVPWs), 8.6 mm ± 1.7; and fractional shortening (FS), 40.7% ± 7.4. Consistent with our previous study reporting that echo abnormalities become evident from around 21 mo of age (21), the measured values of those items in the two dogs after four PPMO injections were also in the normal range: LVIDd, 24.5 mm ± 0.7; LVIDs, 14.7 mm ± 0.5; IVSd, 6.5 mm ± 0.7; IVSs, 10.0 mm ± 1.4; LVPWd, 7.5 mm ± 0.7; LVPWs, 10.5 mm ± 0.7; and FS, 37.0% ± 1.4. Obvious abnormality in heart rate was not observed in all PPMO-treated dogs during the course of monitoring (Fig. S3).

Toxicology. Blood tests examining possible side effects of the 3-PPMO cocktail (total 12 mg/kg, i.v.) showed no obvious abnormalities related to hepatic or renal damage, electrolyte imbalance, or anemia due to systemic treatment in all dogs tested: dogs 5301FA and 5306MA were subjected to four i.v. injections and dog 3905FA was treated with a single i.v. injection (Fig. S4). A transient increase in some hepatic indicators (aspartate aminotransferase and alanine aminotransferase) was observed in dog 5301FA; total bilirubin was also transiently increased in dog 5306MA. However, levels of a more specific indicator of liver damage, gamma-glutamyltransferase, were less than 3 IU/L within the normal range (0–10 IU/L in healthy beagle dogs at <1 y of age) throughout the monitoring period of all i.v.-treated dogs (29). Transiently elevated levels of blood urea nitrogen and creatinine, indicative of renal damage, were detected in dog 5306MA following the second i.v. injection, but that was reduced after the third injection. No obvious reduction of creatine kinase levels was observed in the treated CXMD$_J$ dogs.

As peptides have the potential to become antigens, we examined the susceptibility of the 3-PPMO cocktail to cause immune activation by counting leukocyte numbers in systemically treated dogs. During systemic treatment, the number of white blood cells, leukocytes, and monocytes did not show any apparent changes with PPMO injection frequency (Fig. S5 *A–C*). The number of CD3-positive T leukocytes as detected by immunohistochemistry was also not obviously altered in both skeletal and cardiac muscles of three i.v.-treated dogs 2 wk after the injection compared with the nontreated group, indicating that systemic treatment with the 3-PPMO cocktail induces little or no immune activation (Fig. S5 *D* and *E*).
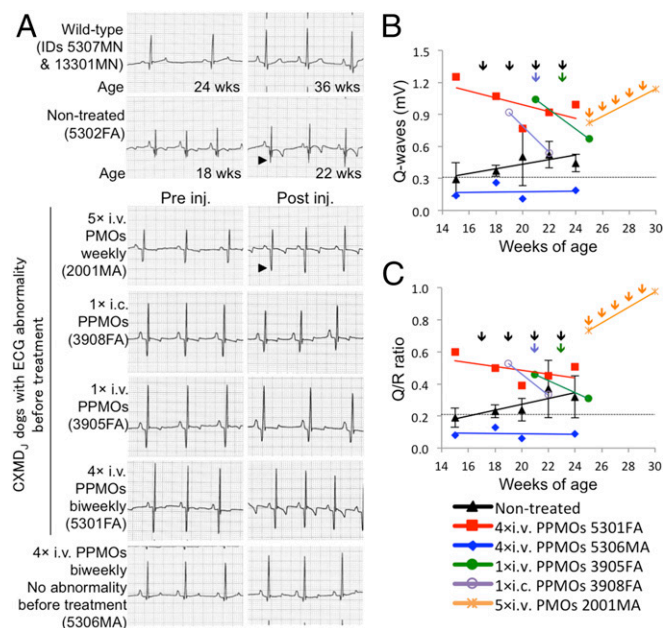
Concentrations of 3-PPMOs in Serum and Tissue Lysate from i.v.-Treated Dystrophic Dogs. Concentrations of the three i.v.-injected PPMOs (Ex6A, Ex6B, or Ex8A PPMO, 4 mg/kg/PPMO/injection) in serum, liver, skeletal, and cardiac muscles were measured by ELISA using PPMO-specific DNA probes (Fig. S6A). Although no PPMOs were detected before the injection, the increased blood concentration of each PPMO was observed 24 h after every i.v. injection (except the second injection in dog 5301FA). A certain level of all 3-PPMOs was maintained throughout the treatment in i.v.-treated dogs regardless of injection frequency (Fig. S6B). After the final injection, the blood levels of individual PPMOs were uniformly and gradually reduced over time, with detectability persisting up to at least 2 wk later. We also found that all 3-PPMOs were detectable at comparable levels in skeletal and cardiac muscles collected 2 wk after the final injection (Fig. S6C), whereas no PPMOs were detected in muscles of nontreated dogs. The finding indicates that simultaneously injected different PPMOs can be evenly distributed to both skeletal and cardiac muscles regardless of muscle type and position (e.g., left and right ventricles and interventricular septum represented in

Fig. 5. Electrocardiogram changes after treatment with 3-PPMO cocktail at 12 mg/kg/injection. (*A*) Electrocardiogram in CXMD$_J$ dogs 2 wk pre- and post-treatment with the PPMO cocktail by a single i.c. or i.v. injection, and by four consecutive i.v. injections. Arrowheads indicate an increase in Q-amplitude. Paper speed, 50 mm/s. Changes of Q-waves (*B*) and Q/R ratio (*C*) by treatment with the cocktail of PPMOs. Three nontreated affected dogs (mean ± SEM) and one affected dog i.v.-treated with the 3-unmodified PMO cocktail (120 mg/kg in total) five times at 1-wk intervals are shown as negative controls. Colored lines indicate linear approximations of the plots. Dotted lines indicate the average values observed in wild-type dogs (*n* = 6).

PPMO accumulation in the liver was observed at much higher levels compared with the muscles in the three treated dogs.

Discussion

The incidence of cardiomyopathy in DMD patients is estimated to be ~59% by 10 y of age (1), and almost 100% of patients exhibit some cardiac involvement by 18 y (30). Cardiac failure causes mortality in 12–20% of DMD patients (26, 31). As demonstrated in clinical trials and in many animal studies, PMO is a promising chemistry for exon-skipping therapy, especially in terms of its safety and sufficient effectiveness in skeletal muscles. However, systemic treatment using PMOs has induced barely detectable dystrophin protein levels in the myocardium of DMD animal models (10, 11, 32). The reasons for the observed variations in PMO efficacy between skeletal and cardiac muscles are largely unknown. To increase therapeutic potency in cardiac muscle, CPP-conjugated PMOs have been developed. Although PPMO efficacy varies depending on peptide components of PPMOs (18), systemic PPMO treatment has consistently induced high-efficiency production of truncated dystrophin protein in bodywide muscles of *mdx* mice, including the heart (17, 33). However, it remains to be determined if systemic injections with PPMOs could rescue expression of dystrophin protein in both skeletal and cardiac muscles of large animal models. In the present study, although low levels of rescued dystrophin protein were observed, systemic multiexon skipping using a 3-PPMO cocktail at 12 mg/kg restored dystrophin expression in skeletal and cardiac muscles of CXMD$_J$ dogs in which dystrophin protein is normally undetectable. As assessed by Western blotting, the quantity of rescued dystrophin protein was not as high as expected in both skeletal and cardiac muscles of the CXMD$_J$ dogs treated with systemic 3-PPMO injections, considering that previous studies in *mdx* mice showed dystrophin rescue to levels comparable to those of wild-type mice (17, 33). This variation may be due to the difficulty of skipping multiple exons (8) or to differences in experimental conditions, such as using a lower dose of 4 mg/kg for each PPMO (as in the present study) compared with a previous report of single exon skipping using a PPMO at 30 mg/kg administrated through i.v. injections in mice (17). Despite overall low levels of dystrophin rescue in CXMD$_J$ dogs, the fact that we observed nearly equal dystrophin levels between the skeletal and cardiac muscles indicates that the peptide B modification can enhance the efficacy of SSOs in the myocardium of dystrophin-deficient dogs.

Another considerable concern in the present study is that no improvement of clinical grading scores and functions was found in skeletal muscles of CXMD$_J$ dogs consecutively treated with the 3-PPMO cocktail at 12 mg/kg/injection. The failure of restoring skeletal muscle function may relate to the time of initiation of therapy. Unlike with DMD mouse models, dystrophic dogs exhibit progressive degeneration and clinical symptoms in skeletal muscles from the neonatal period (12). In this study, we began the treatment of affected dogs at 4 mo of age when the cardiac abnormalities became evident on ECG. The present finding suggests the need for starting PPMO treatment at younger ages to restore skeletal muscle functions in the dystrophic dog model. Also, it has been reported that rescue of more than 10% of normal dystrophin levels is required for functional recovery in skeletal muscle of a dystrophic mouse model (32). However, a recent clinical trial with an exon 51-skipping PMO antisense drug has had an encouraging result: very low to undetectable levels of rescued dystrophin protein in Western blotting analysis can help slow a decline in walking ability of DMD patients subjected to treatment with a single weekly i.v. injection over a span of 3 y (3). One implication from the clinical trial is that low expression levels of dystrophin (~5% compared with healthy dogs) might have a potential for leading to some clinical benefit in skeletal muscles in long-term treatment.

DMD/BMD-associated cardiomyopathy includes various cardiac arrhythmias, as represented by ECG, implicating dysfunction of the cardiac conduction system. In fact, dystrophin-deficient Purkinje fibers have been reported to exhibit vacuole degeneration in patients with DMD (24, 31) and in CXMD$_J$ dogs (22). We previously described overexpression of a dystrophin short isoform, Dp71, in the Purkinje fibers of CXMD$_J$ dogs (22). However, the excess Dp71 expression does not compensate for a lack of the Dp427m (full-length) isoform in CXMD$_J$ dogs. The rescue of full-length dystrophin (with exons 6–9 skipping) in Purkinje fibers could ameliorate or prevent cardiac arrhythmias in DMD patients. Our results support this hypothesis: the 3-PPMO cocktail administration ameliorated abnormally deep Q-waves and increased Q/R ratio in three CXMD$_J$ dogs. These improvements appear to be associated with expression of the rescued full-length dystrophin protein and the amelioration of vacuole degeneration in Purkinje fibers.

In association with our observations of dystrophin rescue in PPMO-treated dog hearts, it has been reported that as little as <2% rescued dystrophin (compared with normal levels), as represented by Western blotting, improves cardiac function in a dystrophic mouse model (32). Also, unlike the working myocardium, expression of dystrophin-associated proteins, such as sarcoglycans and β-dystroglycan, is well maintained in the Purkinje fibers of CXMD$_J$ dogs (22). Dystrophin-deficient heart, which is more mildly affected than skeletal muscles, might retain the potential to work normally if the cardiac conduction system can be improved with the rescue of full-length dystrophin. To examine this possibility, further studies are required with more optimized regimens for PPMO treatment in the dog model, such as dosages and routes of PPMO administration and injection frequencies. Nevertheless, the present findings suggest that dystrophin Dp427m plays an important role in maintaining the normal architecture and function of the cardiac Purkinje fibers.

As represented here, exon skipping with PPMOs can more effectively restore dystrophin expression in skeletal and cardiac muscles and ameliorate abnormalities of the cardiac conduction system in dystrophic animal models compared with unmodified morpholinos (10, 16, 34). However, higher toxicity is a major concern in the use of the PPMO chemistry (35). There was no obvious toxicity or immune response detected by blood tests, histological assessment, and antibody tests in *mdx* mice systemically injected with 30 mg/kg peptide B-conjugated PMO at 2-wk intervals for 3 mo (17) and at 1-mo intervals for 1 y (33). Tolerance to other arginine-rich CPPs has also been reported at up to 30 mg/kg in *mdx* mice with no apparent signs of toxicity (35, 36). Although the population of dogs used in this study is limited, our regimen involving a single i.v. injection and four i.v. injections at 2-wk intervals with the 3-PPMO cocktail (12 mg/kg/injection, 4 mg/kg each) showed no obvious toxic effects in blood tests. An important finding in the present safety assessment is that residual PPMOs as detected by ELISA after the final injection did not induce adverse effects detectable in blood tests up to 2 wk later. We also found no apparent signs of immune activation as detected by leukocyte counts. However, a challenge to verify antibody production against CPPs remains to be resolved. Along with the effectiveness of PPMO-mediated multiple exon skipping, studies on the long-term safety of the PPMO chemistry need to be further pursued with various doses and frequencies. A current challenge in studies with PPMOs is the limitation of manufacturing sufficient PPMO amounts for large animal models as found in the present study using three different PPMOs. As PPMOs have high potential to treat DMD, particularly the heart, and to become a promising clinical drug candidate in exon skipping, this issue needs to be overcome before clinical trials begin.

In conclusion, we have demonstrated the efficacy of multiexon skipping, using a 3-PPMO cocktail, in rescuing dystrophin protein expression in the cardiac muscles and bodywide skeletal muscles

MEDICAL SCIENCES

of a dystrophic dog model. In addition, we found that rescued dystrophin protein in cardiac Purkinje fibers could contribute to the improvement or prevention of conduction abnormalities in the dystrophic heart. The present preclinical data provide valuable information for translational research toward future human clinical trials involving exon-skipping therapy with PPMOs.

Materials and Methods

Detailed descriptions of animal PPMOs and PMOs, injections of PPMOs and PMOs, clinical evaluation, locomotor activity assay, RT-PCR, immunohistochemistry, H&E staining, Western blotting, ECG, echo, blood tests, blood cell counting, and ELISA are provided in *SI Materials and Methods*.

All experimental procedures were approved by the Institutional Animal Experiment Committees of the National Center of Neurology and Psychiatry. All methods were performed according to the approved guidelines and under the supervision of veterinarians.

1. Flanigan KM (2014) Duchenne and Becker muscular dystrophies. *Neurol Clin* 32(3): 671–688, viii.
2. Koenig M, et al. (1987) Complete cloning of the Duchenne muscular dystrophy (DMD) cDNA and preliminary genomic organization of the DMD gene in normal and affected individuals. *Cell* 50(3):509–517.
3. Mendell JR, et al.; Eteplirsen Study Group and Telethon Foundation DMD Italian Network (2016) Longitudinal effect of eteplirsen versus historical control on ambulation in Duchenne muscular dystrophy. *Ann Neurol* 79(2):257–271.
4. Echigoya Y, Mouly V, Garcia L, Yokota T, Duddy W (2015) In silico screening based on predictive algorithms as a design tool for exon skipping oligonucleotides in Duchenne muscular dystrophy. *PLoS One* 10(3):e0120058.
5. Béroud C, et al. (2007) Multiexon skipping leading to an artificial DMD protein lacking amino acids from exons 45 through 55 could rescue up to 63% of patients with Duchenne muscular dystrophy. *Hum Mutat* 28(2):196–202.
6. Nakamura A, et al. (2016) Deletion of exons 3-9 encompassing a mutational hot spot in the DMD gene presents an asymptomatic phenotype, indicating a target region for multiexon skipping therapy. *J Hum Genet* 61(7):663–667.
7. Aartsma-Rus A, et al. (2009) Theoretic applicability of antisense-mediated exon skipping for Duchenne muscular dystrophy mutations. *Hum Mutat* 30(3):293–299.
8. Echigoya Y, Yokota T (2014) Skipping multiple exons of dystrophin transcripts using cocktail antisense oligonucleotides. *Nucleic Acid Ther* 24(1):57–68.
9. Aoki Y, et al. (2012) Bodywide skipping of exons 45-55 in dystrophic mdx52 mice by systemic antisense delivery. *Proc Natl Acad Sci USA* 109(34):13763–13768.
10. Yokota T, et al. (2009) Efficacy of systemic morpholino exon-skipping in Duchenne dystrophy dogs. *Ann Neurol* 65(6):667–676.
11. Aoki Y, et al. (2010) In-frame dystrophin following exon 51-skipping improves muscle pathology and function in the exon 52-deficient mdx mouse. *Mol Ther* 18(11): 1995–2005.
12. Yu X, Bao B, Echigoya Y, Yokota T (2015) Dystrophin-deficient large animal models: Translational research and exon skipping. *Am J Transl Res* 7(8):1314–1331.
13. Alter J, et al. (2006) Systemic delivery of morpholino oligonucleotide restores dystrophin expression bodywide and improves dystrophic pathology. *Nat Med* 12(2): 175–177.
14. Kornegay JN, et al. (2010) Widespread muscle expression of an AAV9 human minidystrophin vector after intravenous injection in neonatal dystrophin-deficient dogs. *Mol Ther* 18(8):1501–1508.
15. Yue Y, et al. (2015) Safe and bodywide muscle transduction in young adult Duchenne muscular dystrophy dogs with adeno-associated virus. *Hum Mol Genet* 24(20): 5880–5890.
16. Jearawiriyapaisarn N, Moulton HM, Sazani P, Kole R, Willis MS (2010) Long-term improvement in mdx cardiomyopathy after therapy with peptide-conjugated morpholino oligomers. *Cardiovasc Res* 85(3):444–453.
17. Wu B, et al. (2008) Effective rescue of dystrophin improves cardiac function in dystrophin-deficient mice by a modified morpholino oligomer. *Proc Natl Acad Sci USA* 105(39):14814–14819.
18. Jearawiriyapaisarn N, et al. (2008) Sustained dystrophin expression induced by peptide-conjugated morpholino oligomers in the muscles of mdx mice. *Mol Ther* 16(9):1624–1629.
19. Crisp A, et al. (2011) Diaphragm rescue alone prevents heart dysfunction in dystrophic mice. *Hum Mol Genet* 20(3):413–421.
20. Willmann R, Possekel S, Dubach-Powell J, Meier T, Ruegg MA (2009) Mammalian animal models for Duchenne muscular dystrophy. *Neuromuscul Disord* 19(4):241–249.
21. Yugeta N, et al. (2006) Cardiac involvement in Beagle-based canine X-linked muscular dystrophy in Japan (CXMDJ): Electrocardiographic, echocardiographic, and morphologic studies. *BMC Cardiovasc Disord* 6:47.
22. Urasawa N, et al. (2008) Selective vacuolar degeneration in dystrophin-deficient canine Purkinje fibers despite preservation of dystrophin-associated proteins with overexpression of Dp71. *Circulation* 117(19):2437–2448.
23. Sanyal SK, Johnson WW (1982) Cardiac conduction abnormalities in children with Duchenne's progressive muscular dystrophy: Electrocardiographic features and morphologic correlates. *Circulation* 66(4):853–863.
24. Nomura H, Hizawa K (1982) Histopathological study of the conduction system of the heart in Duchenne progressive muscular dystrophy. *Acta Pathol Jpn* 32(6):1027–1033.
25. Moise NS, et al. (1991) Duchenne's cardiomyopathy in a canine model: Electrocardiographic and echocardiographic studies. *J Am Coll Cardiol* 17(3):812–820.
26. Finsterer J, Stöllberger C (2003) The heart in human dystrophinopathies. *Cardiology* 99(1):1–19.
27. Spurney CF (2011) Cardiomyopathy of Duchenne muscular dystrophy: Current understanding and future directions. *Muscle Nerve* 44(1):8–19.
28. Crippa L, Ferro E, Melloni E, Brambilla P, Cavalletti E (1992) Echocardiographic parameters and indices in the normal beagle dog. *Lab Anim* 26(3):190–195.
29. Braun JP, Benard P, Burgat V, Rico AG (1983) Gamma glutamyl transferase in domestic animals. *Vet Res Commun* 6(2):77–90.
30. Nigro G, Comi LI, Politano L, Bain RJ (1990) The incidence and evolution of cardiomyopathy in Duchenne muscular dystrophy. *Int J Cardiol* 26(3):271–277.
31. Yanagisawa A, et al. (1992) The prevalence and prognostic significance of arrhythmias in Duchenne type muscular dystrophy. *Am Heart J* 124(5):1244–1250.
32. Wu B, et al. (2011) One-year treatment of morpholino antisense oligomer improves skeletal and cardiac muscle functions in dystrophic mdx mice. *Molecular Ther* 19(3): 576–583.
33. Wu B, et al. (2012) Long-term rescue of dystrophin expression and improvement in muscle pathology and function in dystrophic mdx mice by peptide-conjugated morpholino. *Am J Pathol* 181(2):392–400.
34. Moulton HM, Moulton JD (2010) Morpholinos and their peptide conjugates: Therapeutic promise and challenge for Duchenne muscular dystrophy. *Biochim Biophys Acta* 1798(12):2296–2303.
35. Amantana A, et al. (2007) Pharmacokinetics, biodistribution, stability and toxicity of a cell-penetrating peptide-morpholino oligomer conjugate. *Bioconjug Chem* 18(4): 1325–1331.
36. Betts C, et al. (2012) Pip6-PMO, a new generation of peptide-oligonucleotide conjugates with improved cardiac exon skipping activity for DMD treatment. *Mol Ther Nucleic Acids* 1:e38.
37. Yokota T, et al. (2012) Extensive and prolonged restoration of dystrophin expression with vivo-morpholino-mediated multiple exon skipping in dystrophic dogs. *Nucleic Acid Ther* 22(5):306–315.
38. Hayashita-Kinoh H, et al. (2015) Intra-amniotic rAAV-mediated microdystrophin gene transfer improves canine X-linked muscular dystrophy and may induce immune tolerance. *Mol Ther* 23(4):627–37.
39. Echigoya Y, et al. (2015) Long-term efficacy of systemic multiexon skipping targeting dystrophin exons 45-55 with a cocktail of vivo-morpholinos in mdx52 mice. *Mol Ther Nucleic Acids* 4:e225.
40. Hally AD (1964) A counting method for measuring the volumes of tissue components in microscopical sections. *J Cell Sci* s3(105):503–517.
41. Burki U, et al. (2015) Development and application of an ultrasensitive hybridization-based ELISA method for the determination of peptide-conjugated phosphorodiamidate morpholino oligonucleotides. *Nucleic Acid Ther* 25(5):275–284.
42. Osborne BE, Leach GD (1971) The beagle electrocardiogram. *Food Cosmet Toxicol* 9(6):857–864.
43. Matsuzawa T, Nomura M, Unno T (1993) Clinical pathology reference ranges of laboratory animals. Working Group II, Nonclinical Safety Evaluation Subcommittee of the Japan Pharmaceutical Manufacturers Association. *J Vet Med Sci* 55(3):351–362.
44. Wolford ST, et al. (1986) Reference range data base for serum chemistry and hematology values in laboratory animals. *J Toxicol Environ Health* 18(2):161–188.
45. Aiello SE, Moses MA (2016) *The Merck Veterinary Manual*, Online Edition (Merck, Kenilworth, NJ).